J Mol Model (2010) 16:1179–1186
DOI 10.1007/s00894-009-0631-x

ORIGINAL PAPER

Density functional studies of the substituent effect on absorption and emission properties of 1, 8-naphthalimide derivatives

Qi Qi · Yongquan Ha · Yueming Sun

Received: 13 September 2009 / Accepted: 23 November 2009 / Published online: 15 December 2009

Abstract Using TD-PBE1PBE/6-31G* and TD-B3LYP/6-31G* approaches, we calculated the absorption and emission spectra of 1,8-naphthalmide derivatives in gas-phase. The geometric structures optimized by HF/6-31G* and B3LYP/6-31G* models and the absorption and emission maxima were in good agreement with existed experimental measurements. It was also found that the lowest singlet states corresponded mainly to the electronic transition from the highest occupied orbital (HOMO) to the lowest unoccupied molecular orbital (LUMO). Intramolecular charge transfer occurred between substituents and naphthalimic rings. Study also showed that most compounds with low absorption excitation energies had low vertical ionization potentials. Finally, the delocalization electronic energies between substituents and naphthalimic rings of isomers were investigated to obtain further sight into their stability.

Keywords Absorption spectra · DFT · Emission spectra · Frontier molecular orbitals · Isomeric structures · 1,8-Naphthalimide derivatives

Introduction

1,8-naphthalimide derivatives are of immense interest both for intrinsic scientific challenges they pose and for potential applications, particularly for the luminescence properties in visible light scope. High electron affinity [1], wide gap [2, 3], and low reduction potential [4], make them good candidates in organic light-emitting diodes (OLEDs) as n-type materials [5]. They also have applications ranging from sensitizer for Grätzel solar cell [6, 7], to logic gate [8], sensor [9] and charge separation mimic [10], where they act as electron acceptor [11, 12], electron donor [10] or energy donor [13]. Besides, they are also employed as connected units in dendrimers and solvatochromic fluorophores to study dynamic protein interactions [14].

Although research concerning those derivatives have explained numerous phenomena and pushed forward their applications in terms of experimental properties, new challenges are still on the horizon concomitant with stimulus searching for innovated and more efficient dyes and chromophores. On the other hand, present experimental phenomena always give rise to some unexpected problems.

It is reported that 1,8-naphthalimide derivatives substituted at 4-position have high fluorescence quantum yield [15]. A series of 1,8-naphthalimide derivatives are synthesized with substituents in the 4 or 5 position such as oxadiazolyl [16], diphenylamino [17], dimethylamino, amino [18]. The oxadiazolyl isomers show almost analogue absorption and emission maxima [16]. Whereas, 1,8-naphthalimide derivatives, substituted by diphenylamino either in the 4 or 5 position, show distinctive absorption and emission maxima [17]. Isomers' absorption and emission properties substituted with dimethylamino, amino and imidazolyl, pyrazolyl, pyrrolyl in their 4 or 5 position are still unknown.

To the best of our knowledge, theoretical calculations always play an important role in understanding and predicting luminescent properties of organic materials. Some *semi*-empirical approaches and DFT models have been reported for naphthalimide derivatives [19–22]. In the present work, our aim is to investigate the vertical

Electronic supplementary material The online version of this article (doi:10.1007/s00894-009-0631-x) contains supplementary material, which is available to authorized users.

Q. Qi · Y. Ha · Y. Sun (✉)
College of Chemistry and Chemical Engineering,
Southeast University,
Nanjing 211189, People's Republic of China
e-mail: sun@seu.edu.cn

excitation energies for 1,8-naphthalimide derivatives in the presence of diphenylamino, dimethylamino, amino (non-cyclic substituents) and oxadiazolyl, imidazolyl, pyrazolyl and pyrrolyl (heterocyclic substituents). Their electronic interaction energies between substituents and naphthalimic moieties are also analyzed. In order to reduce the systematical deviation, they have been investigated using TD-PBE1PBE/6-31G* and TD-B3LYP/6-31G* models for comparison.

Computation methods

All calculations have been carried out with Gaussian03 suite of programs [23], and with no imaginary frequency in order to ensure numerically accurate results. We have selected the parameter-free PBE1 hybrid functional [24, 25] and B3LYP [26, 27] for all DFT and TD-DFT simulations. 6-31G* basis sets have been used. The ground state (S_0) and the first singlet excited state (S_1) have been optimized for these derivatives with no symmetry constraint. These minimizations have been performed with the HF (S_0), B3LYP (S_0), CIS (S_1) approaches. For all schemes, S_0 states have been confirmed by determination of the vibration frequencies. Vertical ionization potentials (VIP) are calculated by subtracting the total energies of the neutral molecules from the charged molecules at neutral equilibrium geometries. Natural population analysis [28, 29] and natural bond orbitals [30] are carried out to compute atomic charges and interaction energies. The nature of electronic delocalization between the substituent and naphthalimic ring is also quantitatively determined by the NBO3.1 program [31] contained in the Gaussian package. They are obtained by subtracting the energies of the natural Lewis structure with their original ground state energies.

Results and discussion

Geometries of 1,8-naphthalimide derivatives in the S_0 and S_1 states

1,8-naphthalimide derivatives can be treated as a combination of three subsystems; viz. benzene (BN) moiety in the top position, naphthalimide (NI) moiety in the middle position and substituent -R (SU) at the bottom position, as shown in Fig. 1. Substituents are classified into the non-cyclic and the heterocyclic ring moieties. NI and BN moieties are in the rigid naphthalimic plane, as illustrated in Fig. 1. Note that the photophysical properties and the color characteristics of 1,8-naphthalimide derivatives can be rationalized in terms of the molecular polarization. Charges of naphthalimic rings are listed in Table 1, which might reflect the polarization of the molecules.

Table 1 also summarizes selected optimized bond lengths and bond angles at HF/6-31G* and CIS/6-31G* levels. Some N30(C)–C4 (5) and C=O bond distances determined by the X-ray structural analysis are listed in bold [17]. The ground state geometries are investigated by the B3LYP/6-31G* method also, shown in the supplemental material. The HF and B3LYP models predict slightly longer bond lengths than the experimental measurements, which is partly due to solid state effect [32].

Figure 1 illustrates the scheme and bond labels used in Table 1. Comparison of the S_0 and S_1 geometries indicates the contraction of the N30(C)—C4 (5) bond between SU and NI moieties. The interaction between SU and NI in the S_1 state thus strengthens to some extent. The contraction of the dihedrals between SU and NI moieties occurs from S_0 to S_1 state. Small elongation of C=O bond lengths is found in the NI moiety. Few conformation changes occur on the rigid NI moiety. Due to the replacement of N atom with C atom, the oxadiazolyl derivatives keep rigid coplanar geometries. N atoms in the amino and dimethylamino derivatives keep a similar hybrid pattern as that of NH_3. So their dihedrals do not list. Except the oxadiazolyls, the aminos and the dimethyl derivatives, dihedrals of those that rest in the 4-position change more in quantities from S_0 to S_1 than those of the 5-positions.

It is well known that, due to the neglect of electronic correlation, HF and CIS methods may induce fatal error. As shown above, geometrical deviation between the HF and B3LYP models is almost negligible. CIS results are in good agreement with those of the analytical gradient from DFT [19]. On the other hand, here we care about the relative conformation change from the ground state to the excited state using similar methods. Above limitation will be reduced.

Table 1 also shows calculated atomic partial charges (NBO) of the S_0 and S_1 state at HF/6-31G* and CIS/6-31G* levels. Positive charges of the connected carbon atoms (C4) in 4-position isomers increase from S_0 to S_1

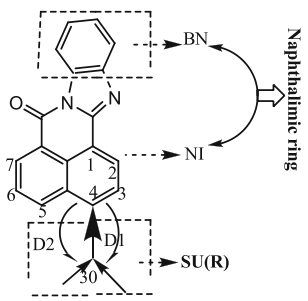

R= oxadiazolyl, imidazolyl, pyrazolyl, pyrrolyl, diphenylamino [-N(Ph)$_2$], dimethylamino [-N(Me)$_2$], amino (-NH$_2$), hydrogen (H) R in 4 or 5 position

Da=1/2(D2+D1)

Fig. 1 The structure and numbering of 1, 8-naphthalimide derivatives

Table 1 Optimized bond lengths (nm), bond angle, dihedrals, NBO charge (a.u.) and dipole (debye) of 1, 8-naphthalimide derivatives at HF/6-31G* and CIS/6-31G* levels

Substituents	4-NH_2	5-NH_2	4-$N(Me)_2$	5-$N(Me)_2$	4-$N(Ph)_2$	5-$N(Ph)_2$	H	
B2/(nm)	0.139	0.138	0.142	0.141	0.142 **0.142**	0.142 **0.142**	——	
B1/(nm)	0.119	0.120	0.119	0.119	0.119	0.119	0.119	
q_O/(a.u.)	−0.685	−0.692	−0.683	−0.698	−0.682	−0.684	−0.680	
q_{C4}/(a.u.)	0.285	−0.166	0.248	−0.162	0.237	−0.158	−0.168	
q_{C5}/(a.u.)	−0.146	0.306	−0.144	0.300	−0.140	0.258	−0.149	
q_{NI} /(a.u.)	0.078	0.066	0.135	0.107	0.175	0.168	——	
Da /(°)	——	——	——	——	58.5 **55.6**	56.6 **53.5**	——	
B2/(nm)	0.135	0.135	0.139	0.140(7)	0.139	0.139	——	
B1/(nm)	0.120	0.120	0.120	0.120	0.123	0.120	0.119	
q_O/(a.u.)	−0.713	−0.700	−0.707	−0.701	−0.725	−0.701	−0.702	
q_{C4}/(a.u.)	0.292	−0.212	0.258	−0.175	0.213	−0.186	−0.167	
q_{C5}/(a.u.)	−0.247	0.303	−0.217	0.236	−0.199	0.211	−0.193	
q_{NI} /(a.u.)	−0.006	0.008	0.061	0.122	0.034	0.048	——	
Da /(°)	——	——	——	——	48.0	50.4	——	
Substituents	4-oxadiazolyl	5-oxadiazolyl	4-imidazolyl	5-imidazolyl	4-pyrazolyl	5-pyrazolyl	4-pyrrolyl	5-pyrrolyl
B2/(nm)	0.147	0.148	0.142	0.142	0.142	0.141	0.142	0.141
B1/(nm)	0.119	0.119	0.119	0.119	0.119	0.119	0.119	0.119
q_O/(a.u.)	−0.677	−0.675	−0.676	−0.676	−0.679	−0.680	−0.678	−0.679
q_{C4}/(a.u.)	−0.093	−0.173	0.204	−0.175	0.225	−0.155	0.220	−0.170
q_{C5}/(a.u.)	−0.154	−0.074	−0.155	0.226	−0.137	0.255	−0.151	0.244
q_{NI} /(a.u.)	0.021	0.015	0.229	0.224	0.222	0.218	0.216	0.209
Da /(°)	0	0	−72.8	−57.7	54.4	−53.2	−67.8	65.9
B2/(nm)	0.145	0.145	0.141	0.141	0.140	0.141	0.140	0.141
B1/(nm)	0.120	0.120	0.120	0.120	0.120	0.120	0.120	0.120
q_O/(a.u.)	−0.690	−0.697	−0.698	−0.699	−0.699	−0.701	−0.700	−0.699
q_{C4}/(a.u.)	−0.081	−0.130	0.218	−0.168	0.227	−0.147	0.235	−0.169
q_{C5}/(a.u.)	−0.165	−0.130	−0.200	0.172	−0.240	0.196	−0.203	0.202
q_{NI} /(a.u.)	0.049	0.064	0.200	0.235	0.187	0.220	0.159	0.205
Da /(°)	0	0	−52.4	−71.4	40.0	−49.0	−47.7	−59.5

The bold values are from X-ray data in the reference [17]. Da=1/2(D2+D1)

state while those (C5) of 5-position isomers decrease. Charges of naphthalimic ring reduce from S_0 to S_1 state, with the exception of the 4-oxadiazolyl, 5-oxadiazolyl, 4-imidazolyl, 5-pyrazolyl derivatives. Except the oxadiazolyls, NBO charges of the naphthalimic rings in 4-position isomers change more than those of 5-position isomers from S_0 to S_1 state. NBO charges of the naphthalimic rings for these non-cyclics diminish in contrast to increased trend of those heterocyclics. The above phenomena show the charge transfer occurs between the naphthalimic ring and the substituent, which is of great essence to improve the excited state properties.

Frontier molecular orbitals (FMOs) analysis

The S_0 state geometries are calculated by B3LYP/6-31G* method while the S_1 state geometries are optimized by CIS/6-31G* method. A graphical display of the FMOs and corresponding energy levels of the S_0 and S_1 state optimized by HF/6-31G* and CIS/6-31G* methods is shown in Fig. 2. FMOs in the top two rows are for HOMOs and LUMOs at HF/6-31G* level. The following two rows are for HOMOs and LUMOs at CIS/6-31G* level.

Frontier molecular orbitals of the S_0 and S_1 state suggest a delocalization distribution of each conjugation subsystem. HOMOs are mainly localized on the rigid naphthalimic ring. HOMO of the 4-oxadiazolyl derivative has a few electron distributions from its oxadiazolyl part while the 5-oxadiazolyl has fewer distributions from its oxadiazolyl part. For HOMOs of the oxadiazolyl derivatives, the imidazolyl derivatives and the like, the heterocyclic components exert a few contributions. Those non-cyclic components exert some contributions in their HOMOs. LUMOs are mainly localized on the NI moiety but leave a

few contributions on the top BN moiety. LUMOs of the oxadiazolyl derivatives are of bonding patterns between naphthalimic rings and substituents. Similar distribution contour for HOMOs and LUMOs of the oxadiazolyl isomers gives rise to similar $S_1 \leftarrow S_0$ excitation properties. LUMOs of those rests are almost with the identical *anti-*bonding patterns. Orbital contour of the oxadiazolyls also suggests the extended rigid geometries of oxadiazolyl in the 4 or 5 positions. For the diphenylamino derivatives, diphenylamino component contributes many to HOMOs but few to LUMOs. Different FMOs of the diphenylaminos suggest their distinctive *singlet-singlet* transition. Distribu-

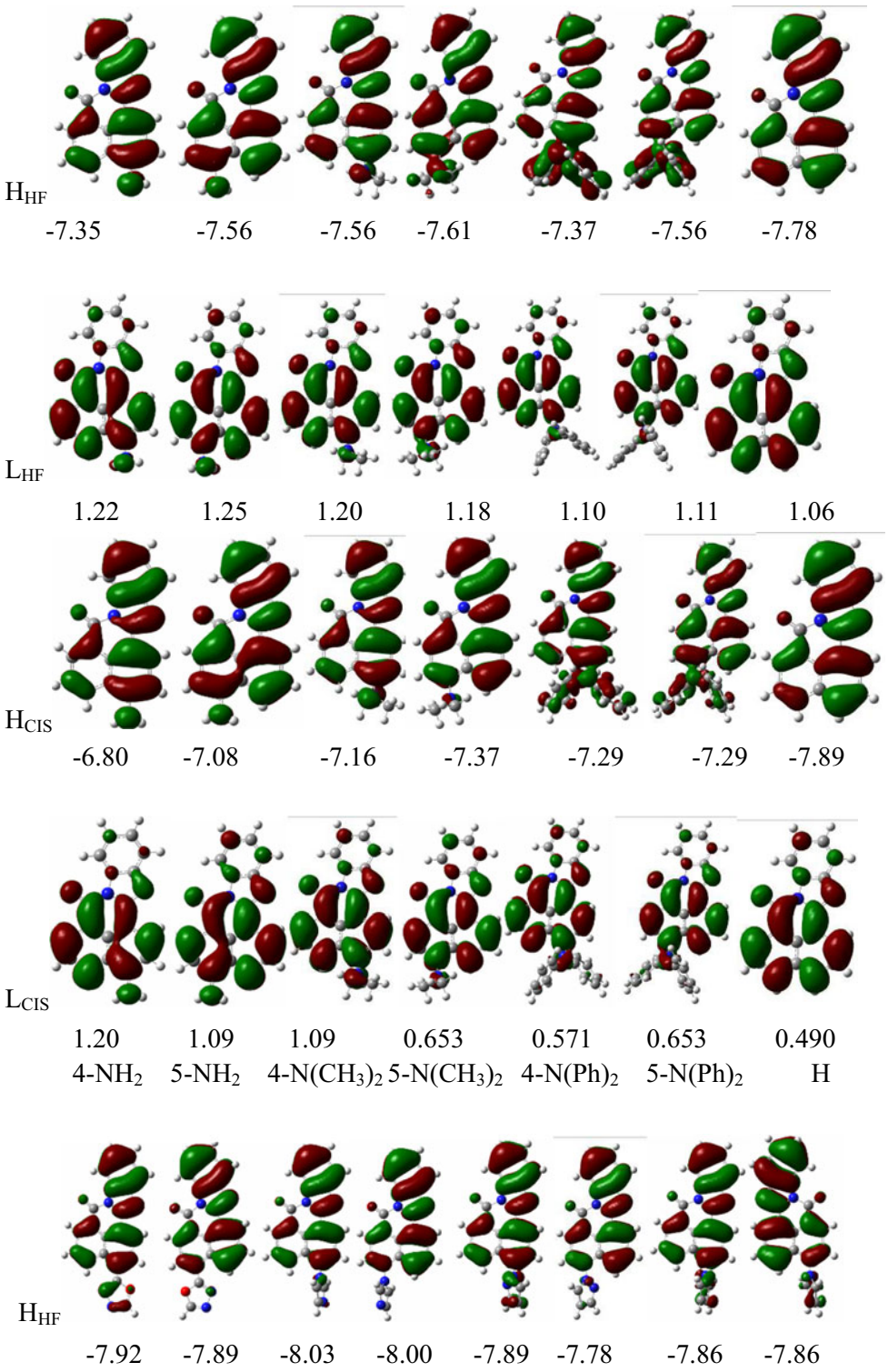

Fig. 2 The contour and energy levels (in eV) of the frontier orbitals of 1,8-naphthalimide derivatives. H(HOMO) L(LUMO)

Fig. 2 (continued)

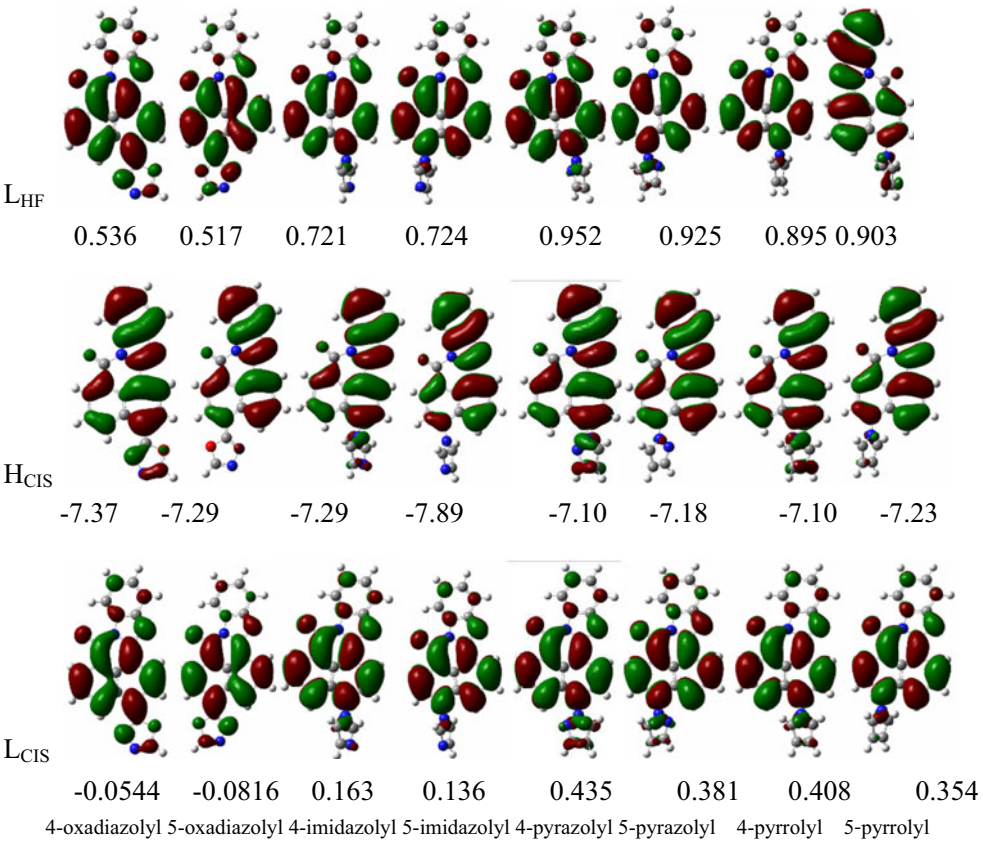

tion patterns on naphthalimic ring of HOMO and LUMO in the 1,8-naphthalimic ring are also similar to the former DFT study [19]. The above studies indicate that the naphthalimic ring is the main chromophore, which may be modified by substituents.

Figure 2 also shows that HOMOs of substituted 1,8-naphthalmic rings have a diminished energy level compared with 1,8-naphthalimide. The heterocyclic derivatives diminish much more than those of non-cyclics. Energy levels of LUMOs for the heterocyclics decrease while those of non-heterocyclics increase. Energy levels of HOMOs increase and those of LUMOs reduce from S_0 to S_1 state. The 4-position isomers have lower energy gaps than those of 5-positions for the non-cyclics. The 4-positions have bigger energy gaps than the 5-positions for the heterocyclics.

Absorption and emission properties

The molecular geometries optimized by B3LYP/6-31G* and HF/6-31G* methods are in good agreement with each other. Here we use the geometries calculated by B3LYP/6-31G* methods. In order to make a further comparison, the vertical absorption transition energies by TD-PBE1PBE/6-31G* are also grounded in the optimized geometries from the B3LYP/6-31G* method, as shown in Table 2.

There are few experimental data concerning these compounds so that we cannot make a direct linear comparison between the experimental values and theoretical values. Our theoretical work is of practical meaning for studying the above compounds from a structural and electronic properties side on the molecular scale. Table 3 gives the calculated emission wavelengths investigated by the TD-PBE1PBE/6-31G* and TD-B3LYP/6-31G* models. The vertical transition energies of some organic molecules calculated by TD-B3LYP/6-31G* approach have a deviation of about 0.25 eV [33]. The vertical absorption and emission electronic transition energies of these compounds calculated by TD-B3LYP/6-31G* method in gas-phase are about 0.1-0.15 eV lower than those obtained by TD-PBE1PBE/6-31G* method in Tables 2 and 3. The vertical excitation energies of the $S_1 \leftarrow S_0$ transition of the diphenylamino isomers from TD-PBE1PBE/6-31G* method are 2.36 eV and 2.49 eV. Compared with experiment values in CH_2Cl_2 [17], both of them are about 0.18 eV lower. The results from TD-PBE1PBE/6-31G* method are in better agreement with the experimental values than TD-B3LYP/6-31G* method. So we calculate the vertical emission electronic transition energy only using TD-PBE1PBE/6-31G* model.

Specifically speaking, the first lowest *singlet-singlet* transition of the absorption and emission transition between

Table 2 Vertical excitation energy (absorption maxima), oscillator strength(f), and main configuration of gas-phase 1, 8-naphthalimide derivatives calculated at TD-B3LYP/6-31G* and TD-PBE1PBE/6-31G*. (Based on the geometries optimized by the B3LYP/6-31G*) (Assignment; H=HOMO, L=LUMO,L+1=LUMO+1, *etc*. E.E (excitation energy))

Gas-phase	Absorption	TD-B3LYP/6-31G*		Gas phase	TD-PBE1PBE/6-31G*	
Substituents	E.E/(eV)	f	Configuration	E.E/(eV)	f	Configuration
4-NH_2	2.70(459)	0.201	H->L 0.647	2.82(440)	0.226	H->L 0.651
5-NH_2	3.08(403)	0.372	H->L 0.636	3.19(389)	0.413	H->L 0.643
4-$N(Me)_2$	2.74(452)	0.270	H->L 0.649	2.85(435)	0.299	H->L 0.653
5-$N(Me)_2$	3.00(413)	0.385	H->L 0.642	3.11(399)	0.433	H->L 0.648
4-$N(Ph)_2$	2.38(521)	0.245	H->L 0.669	2.50(495)	0.309	H->L 0.668
5-$N(Ph)_2$	2.58(480)	0.317	H->L 0.653	2.69(460)	0.347	H->L 0.657
H	2.97(417)	0.232	H->L 0.649	3.10(400)	0.232	H->L 0.649
Gas phase	B-G*		MO character	Gas phase	P-G*	MO character
Substituents	E.E	f	Configuration	E.E	f	Configuration
4-oxadiazolyl	2.82(440)	0.449	H->L 0.634	2.93(423)	0.640	H->L 0.640
5-oxadiazolyl	2.59(479)	0.179	H->L 0.657	2.72(456)	0.206	H->L 0.660
4-imidazolyl	2.86(432(9))	0.287	H->L 0.645	2.99(415)	0.324	H->L 0.650
5-imidazolyl	2.87(432(5))	0.233	H->L 0.647	2.99(414)	0.265	H->L 0.652
4-pyrazolyl	2.89(429)	0.357	H->L 0.646	3.01(412)	0.397	H->L 0.650
5-pyrazolyl	2.86(433)	0.250	H->L 0.649	2.99(415)	0.286	H->L 0.653
4-pyrrolyl	2.80(442)	0.150	H-1->L 0.483	2.94(421)	0.341	H->L 0.642
			H->L 0.481			H-1->L 0.144
5-pyrrolyl	2.85(435)	0.087	H->L -0.431	3.00(413)	0.228	H-1->L −0.326
			H-1->L 0.535			H->L 0.583

the S_0 and S_1 state in gas-phase corresponds to the predominantly electronic transition from HOMO to LUMO. For the diphenylamino isomers in Fig. 2, they have similar HOMO and LUMO distribution on naphthalimic rings but have different electron cloud on their substituents, suggesting different absorption and emission maxima. The 5-position diphenylamino derivative has a stronger oscillator than the 4-position and has higher excitation energies, which is in accordance with experimental measurements [17]. For the oxadiazolyl, imidazolyl, pyrazolyl, pyrrolyl derivatives, these 4-positions have stronger oscillator strength. Bigger dihedrals in Table 1 suggest the lessened electron density overlap between substituted units and naphthalimic units. The heterocyclic plane limits interaction between naphthalimic ring and substituents, which is rather different from the non-cyclics.

Table 3 Vertical excitation energy (emission maxima), oscillator strength(f), and main configuration of 1, 8-naphthalimide derivatives calculated at TD-B3LYP/6-31G* and TD-PBE1PBE/6-31G* levels. (Based on the geometries optimized by the CIS/6-31G*)

Gas phase	emission	TD-B3LYP/6-31G*		Gas	TD-PBE1PBE/6-31G*	
Substituent	E.E	f	Configuration	E.E	f	Configuration
4-NH_2	2.28(544)	0.163	H->L 0.639	2.38(521)	0.183	H->L 0.642
5-NH_2	2.84(436)	0.432	H->L 0.625	2.92(424)	0.457	H->L 0.630
4-$N(Me)_2$	2.40(518)	0.273	H->L 0.633	2.49(498)	0.302	H->L 0.638
5-$N(Me)_2$	2.68(463)	0.364	H->L 0.630	2.78(447)	0.402	H->L 0.636
4-$N(Ph)_2$	2.19(565)	0.379	H->L 0.639	2.29(542)	0.412	H->L 0.643
5-$N(Ph)_2$	2.48(501)	0.459	H->L 0.630	2.56(484)	0.488	H->L 0.636
H	2.60(477)	0.239	H->L 0.630	2.6s0(477)	0.239	H->L 0.635
Gas phase	emission	TD-B3LYP/6-31G*		Gas	TD-PBE1PBE/6-31G*	
Substituent	E.E/(eV)	f	Configuration	E.E/(eV)	f	Configuration
4-oxadiazolyl	2.55(486)	0.503	H->L 0.617	2.640(470)	0.449	H->L 0.623
5-oxadiazolyl	2.23(557)	0.202	H->L 0.641	2.33(531)	0.227	H->L 0.646
4-imidazolyl	2.50(496)	0.334	H->L 0.631	2.50(496)	0.368	H->L 0.636
5-imidazolyl	2.47(501)	0.250	H->L 0.633	2.58(481)	0.277	H->L 0.638
4-pyrazolyl	2.55(487)	0.403	H->L 0.629	2.642(469)	0.440	H->L 0.634
5-pyrazolyl	2.51(494)	0.274	H->L 0.635	2.58(481)	0.277	H->L 0.638
4-pyrrolyl	2.47(502)	0.362	H->L 0.633	2.57(482)	0.396	H->L 0.638
5-pyrrolyl	2.54(488)	0.297	H->L 0.629	.2.65(469)	0.333	H->L 0.637

Table 4 Delocalization energy analysis between naphthalimic rings and substituents of 1, 8-naphthalimide derivatives at HF/6-31G* level

Substituents	4-NH_2	5-NH_2	4-$N(Me)_2$	5-$N(Me)_2$	4-$N(Ph)_2$	5-$N(Ph)_2$	4-Oxadiazolyl	5-Oxadiazolyl	4-Imidazolyl	5-Imidazolyl	4-Pyrazolyl	5-Pyrazolyl	4-Pyrrolyl	5-Pyrrolyl
$\triangle E_{4\text{-}5}$[a] (Hartree)	0.0426		0.0121		0.00566		−0.0329		−0.00916		−0.00937		−0.00358	
$\triangle E$[b] (kcal/mol)	2.80	2.86	2.66	2.73	2.68	2.75	2.60	2.57	2.21	2.24	2.40	2.42	2.26	2.32

[a] $\triangle E_{4\text{-}5}$ stands for the self consistent energy difference between isomers substituted in 4-position and 5-position.

[b] $\triangle E$ symbolizes the stabilization energy difference of the delocalizing contributions between the naphthalimic ring and substituents.

Table 5 Calculated vertical ionization potential (eV) of 1, 8-naphthalimide derivatives

Substituent	4-NH_2	5-NH_2	4-$N(Me)_2$	5-$N(Me)_2$	4-$N(Ph)_2$	5-$N(Ph)_2$	4-Oxadiazolyl	5-Oxadiazolyl	4-Imidazolyl	5-Imidazolyl	4-Pyrazolyl	5-Pyrazolyl	4-Pyrrolyl	5-Pyrrolyl
B2/(eV).	6.79	6.98	6.81	6.95	6.44	6.59	7.36(7)	7.36(6)	7.38	7.43	7.17	7.22	7.12	7.18

Delocalization energy analysis and vertical ionization potentials

On the basis of steric and electrostatic factors, isomers with bigger dihedrals are expected to be significantly more stable, because naphthalimic rings and their substituent are maximally separated in the conformation to reduce their dipoles. This can be verified from the more stable 5-position structures for the diphenylamino derivatives. Table 4 also shows that rest of the non-cyclic derivatives are in favor of the 5-positions. The 4-position heterocyclics are more stable than corresponded 5-positions, which are also partly attributed to the bigger dihedrals in the 4-positions. As seen from Table 4, delocalization energies between SU and NI of the non-cyclics are bigger than those heterocyclics. For the heterocyclics, delocalization energies of the 4 positions are smaller than those of 5 positions except the oxadiazolyls, indicating the 4-positions with smaller dihedrals have smaller delocalization effect between the heterocyclic component and the naphthalimic ring. Delocalization energy reflects the different conformation effect for the heterocyclic and the non-cyclics.

Table 5 summarizes vertical ionization potentials (VIP) of these compounds. For the heterocyclic derivatives, they have higher VIP than those non-cyclics, indicating that those non-cycles have better donating ability. This is in good agreement with their HOMO energy levels. For the non-cyclic derivatives, the 4-position isomers have lower VIP than those 5-positions, which also indicates that these 4-positions are more available for transferring holes. Other than the pyrazolyl, isomers have lower excitation energies when they have lower VIP.

Conclusions

The absorption and emission spectra of 1,8-naphthalmide derivatives in gas-phase have been calculated by using TD-PBE1PBE/6-31G* and TD-B3LYP/6-31G* approaches. The vertical absorption and emission electronic transition energies calculated by means of TD-PBE1PBE/6-31G* method were 0.1~0.15 eV higher than those by means of TD-B3LYP/6-31G* method. Intramolecular charge transfer between the substituents and the naphthalimic rings modified their excitation properties. From S_0 to S_1, the steric degree between substituents and naphthalimic rings reduced. Other than pyrazolyl, isomers with low VIPs have low excitation energies. Delocalization electronic energies of these non-cyclic derivatives were bigger than the heterocyclics. The non-cyclic 1, 8-naphthalimide derivatives are in favor of the 5-positions while the 4-position heterocyclics are more stable than corresponded 5-positions for their 4 and 5 position isomers.

Acknowledgments Authors thank the 973 Program in Natural Basic Research Program of China (2007CB936300), Jiangsu Natural Science Foundation (BK2009293), Changzhou science and technology development planning (CS20090007) and the high performance computation platform of southeast university for supporting this work.

References

1. Cacialli F, Friend RH, Bouche CM, Barny PL, Facoetti H, Soyer F et al. (1998) J Appl Phys 83(4):2343–2356
2. Demeter A, Berces T, Biczok L, Wintgens V, Valat P, Kossanyi J (1996) J Phys Chem 100(6):2001–2011
3. Wintgens V, Valat P, Kossanyi J, Biczok L, Demeter A, Berces T (1994) J Chem Soc Faraday Trans 90(3):411–421
4. Martin E, Weigand R (1998) Chem Phys Lett 288(1):52–58
5. Kolosov D, Adamovich V, Djurovich P, Thompson ME, Adachi C (2002) J Am Chem Soc 124(33):9945–9954
6. Zhu WH, Tian H, Gao EQ, Yang MZ, Klaus L (2000) Chem Lett 29(7):778–779
7. Tian H, Liu PH, Zhu WH, Gao E, Wu DJ, Cai S (2000) J Mater Chem 10(12):2708–2715
8. Lukas AS, Bushard PJ, Wasielewski MR (2001) J Am Chem Soc 123(10):2440–2441
9. Elbert JE, Paulsen S, Robinson L, Elzey S, Klein K (2005) J Photochem Photobiol A 169(1):9–19
10. Le TP, Rogers JE, Kelly LA (2000) J Phys Chem A 104(29):6778–6785
11. Tan Q, Kuciauskas D, Lin S, Stone S, Moore AL, Moore TA et al (1997) J Phys Chem B 101(26):5214–5223
12. Cho DW, Fujitsuka M, Sugimoto A, Yoon UC, Mariano PS, Majima T (2006) J Phys Chem B 110(23):11062–11068
13. Abad S, Kluciar M, Miranda MA, Pischel U (2005) J Org Chem 70(25):10565–10568
14. Loving G, Imperiali B (2008) J Am Chem Soc 130(41):13630–13638
15. Kolosov D, Adamovich V, Djurovich P, Thompson ME, Adachi C (2002) J Am Chem Soc 124(33):9945–9954
16. Zhu WH, Yao R, Tian H (2002) Dyes and Pigments 54(2):147–154
17. Jiang W, Tang J, Qi Q, Sun YM, Ye HY, Fu DW (2009) Dyes and Pigments 80(3):279–286
18. Alexiou MS, Tychopoulos V, Ghorbanian S, Tyman JHP, Brown RG, Brittain PI (1990) J Chem Soc Perk Trans 2(5):837–842
19. Jacquemin D, Perpète EA, Scalmani G, Frisch MJ, Ciofini I, Adamo C (2007) Chem Phys Lett 448(1–3):3–6
20. Miao L, Yao Y, Yang F, Wang Z, Li W, Hu J (2008) THEOCHEM 865:79–87
21. de la Peña O'Shea VA, Pardo AP, Poyato JML (2003) Int J Quantum Chem 91(3):446–450
22. Patsenker LD, Artyukhova YY (2003) J Mol Struct 655(2):311–320
23. Frisch MJ, Trucks GW, Schlegel HB, Scuseria GE, Robb MA, Cheeseman JR et al. (2003) Gaussian03, Revision B.02. Gaussian Inc, Wallingford
24. Elmér R, Berg M, Carlén L, Jakobsson B, Norén B, Oskarsson A et al. (1997) Phys Rev Lett 78(7):1396–1396
25. Perdew JP, Burke K, Ernzerhof M (1996) Phys Rev Lett 77 (18):3865–3868
26. Becke AD (1993) Density-functional thermochemistry. III. The role of exact exchange. J Chem Phys 98(7):5648–5652
27. Miehlich B, Savin A, Stoll H, Preuss H (1989) Chem Phys Lett 157(3):200–206
28. Reed AE, Weinstock RB, Weinhold F (1985) J Chem Phys 83 (2):735–746
29. Reed AE, Weinhold F (1983) J Chem Phys 78(6):4066–4073
30. Foster JP, Weinhold F (1980) J Am Chem Soc 102:7211–7218
31. Reed AE, Glendening ED, Carpenter JE, Weinhold F. Theoretical Chemistry Institute, University of Wisconsin, Madison
32. Jonas V, Frenking G, Manfred Reetz T (1994) J Am Chem Soc 116(19):8741–8753
33. Fabian J (2001) Theor Chem Acc 106(3):199–217